DNA Detection

DOI: 10.1002/anie.200905267

Nanoparticle-Based, Fluorous-Tag-Driven DNA Detection**

*Min Hong, Xin Zhou, Zhiqiang Lu, and Jin Zhu**

Biodiagnostics has been the subject of intense research because of its importance in the identification of infectious agents, diagnosis of disease states, and analysis of forensic samples.[1] A variety of methods have been developed, which rely on the utility of radioactive labels, nonradioactive organic reporter groups, or polymerase chain reactions (PCR), etc.[2–5] Despite the advances, no single approach has excelled in all of the assay attributes, such as sensitivity, selectivity, and practicality. Nanostructures have proven extremely effective in addressing some of the deficiencies associated with conventional technologies.[6,7] In this regard, one area of progress has been the development of straightforward, cost-effective, and instrument-free colorimetric assay systems,[8–11] the versatility and importance of which are exemplified by their applicability to the broad range of target analytes.[12–16] Essentially, these visual inspection schemes take advantage of the distance-dependent variation of localized surface plasmon resonances, and concomitant color change from red to purple/blue in the case of gold nanoparticles (AuNPs). Thus far, ionic and molecular species in solution are exclusively detected with a homogeneous aggregation of heterogeneous nanoparticles in the bulk solution phase. Herein, we report a fundamentally different assay, which relies on the interfacial assembly of nanoparticles. Significantly, with this strategy, AuNP network structures can be created at either the gas/liquid, liquid/liquid, or solid/liquid interface, thereby providing us with the ability to use a single type of architecture for an array of detection formats. Our findings clearly demonstrate the possibility of achieving distinct order in the nanoparticle organizates through the rational design of synthetic assemblers.

For AuNP-based DNA detection, two distinct operating mechanisms (cross-linking and non-cross-linking) have been previously achieved.[8–11] We were intrigued by the possibility of incorporating multiple weak interactions (e.g., unnatural forces besides DNA hybridization) and providing more programmability for the organization of materials. In particular, in the first incarnation of this idea, our system was characterized by the utility of two types of probes, DNA-derivatized AuNPs (DNA–AuNPs) and fluorous-tagged DNA (F–DNA) (Figure 1 A). The target DNA directs placement of F–DNA molecules on the surface of DNA–AuNPs, through sandwich hybridization, leading to the fluorous-tag-driven generation of AuNP polymeric networks at the interface between water and other phases (Figure 1 B,C). Importantly, this enables the visual detection of target DNA either directly in aqueous solution or on a fluorinated substrate surface.

With respect to the controlled assembly of aqueous-dispersed nanoparticles, several unique features distinguish

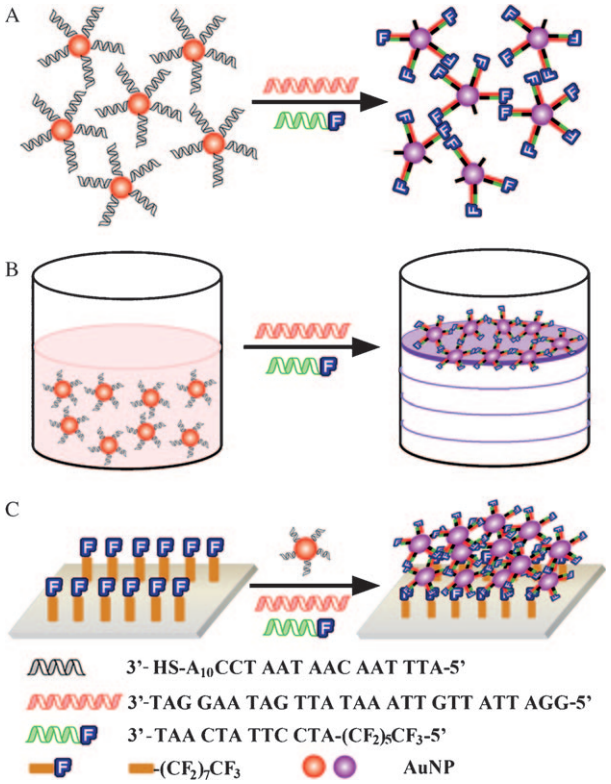

Figure 1. Schematic representation of the DNA detection strategy by interfacial nanoparticle assembly. A) Generation of AuNP network structures through the hybridization of DNA–AuNPs, target DNA, and F–DNA, and fluorous interactions. B) Visual DNA detection by the observation of a purple-colored AuNP thin film formed at the air/water interface. The purple-colored film created at the interface between water and other phases (fluorous solvent and fluorinated solid support) could also be employed for target identification. C) Visual DNA detection by a spot test on a fluorinated substrate (glass slide) (surface-confined and dehydrated AuNP aggregates produced at the solid/water interface). The visualization of AuNP aggregates could be either directly achieved at higher target concentrations or facilitated by the signal amplification at lower target concentrations.

[*] M. Hong, Dr. X. Zhou, Z. Lu, Prof. Dr. J. Zhu
Department of Polymer Science and Engineering
School of Chemistry and Chemical Engineering
State Key Laboratory of Coordination Chemistry
Nanjing National Laboratory of Microstructures
Nanjing University, Nanjing 210093 (China)
Fax: (+86) 25-8331-7761
E-mail: jinz@nju.edu.cn

[**] J.Z. acknowledges support from the National Natural Science Foundation of China (20604011, 20974044, 90923006), National Basic Research Program of China (2007CB925103), New Century Excellent Talents Program in University (NCET-06-0451), and Six-Profession Talents Summit Program of Jiangsu Province (06-A-018).

Supporting information for this article is available on the WWW under http://dx.doi.org/10.1002/anie.200905267.

our system from the previously reported Langmuir monolayer strategy:[17,18] 1) The F–DNA is composed of a long-chain oligonucleotide tail (charged, hydrophilic) and a short-chain fluorous tag head (non-charged, hydrophobic), instead of a large hydrocarbon tail (non-charged, hydrophobic) and a small ionic head (charged, hydrophilic), thereby presenting a new type of building block for structural organization. 2) Programmable, sequence-specific DNA hybridization[19,20] is used to link nanoparticles and a fluorous tag, rather than nondiscriminating electrostatic interactions utilized for other types of entities; 3) the advantage of fluorous-tag-based chemistry over lipid tails is that a single fluorous segment is sufficient to effect the molecular binding, highlighting the extraordinary strength and specificity of this type of interaction.[21–23] Indeed, much shorter carbon chains are required to impart interaction capability for this type of fluorous moieties.[21]

We investigated the AuNP assembly process at the air/water interface. To this end, two sets of probes, as depicted in Figure 1, are essential: DNA–AuNPs, prepared by using the protocol developed by Mirkin and co-workers,[9] and F–DNA, generated by coupling a fluorous-tagged phosphoramidite to the 5′-end of an oligonucleotide (see Figure S1 in the Supporting Information). The DNA portions of these two probes are designed so that they can be recognized sequence specifically and aligned contiguously by the complementary DNA. The proposed method was first tested using a sequence associated with the anthrax lethal factor.[24–26] The solution of DNA–AuNPs (0.3 M PBS buffer: 0.3 M NaCl, 10 mM NaH_2PO_4/Na_2HPO_4, pH 7), after the addition of the target DNA and F–DNA, exhibits a red color at the initial stage. Over time, particle assembly occurs at the air/water interface, accompanied by the eventual formation of a visually observable, purple-colored thin film (Figure 2A). The polymerization of AuNPs and the generation of the purple film are slow processes at room temperature (ca. 25 °C), which is attributable to the steric and charge constraints imposed on the hybridization kinetics by the densely loaded oligonucleotides on the AuNP surfaces. The slow assembly kinetics supports the notion that binding of multiple fluorous tags, through DNA hybridization, is necessary to direct sufficiently hydrophobic AuNPs to the air/water interface. To gain further insight into the dynamic structure, the progression of the AuNP assembly process was monitored by transmission electron microscopy (TEM). Whereas isolated AuNPs dominate at the initial stage (Figure 2B), the aggregated structures start to form over time (see Figure S2 in the Supporting Information). Eventually, the assembly proceeds to completion and extended, quasi-two-dimensional AuNP polymeric networks are generated (Figure 2C), and an extensive amount of local order can be observed (see Figure S3 in the Supporting Information). The DNA layer on the AuNPs prevents fusion among AuNPs in the extended structures, leaving individual particles intact. If one takes out the solution below the purple film, a purple film could again be developed (see Figure S4 in the Supporting Information), revealing the strong cohesive force derived from fluorous interactions. Remarkably, with more uniformly sized AuNPs as building blocks, TEM characterization revealed the existence of not only local order, but also domains of close-packed AuNP assemblies (see Figure S4 in the Supporting Information).

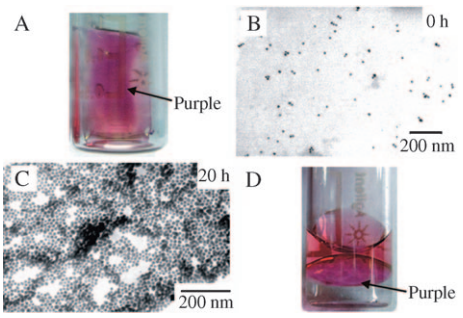

Figure 2. Visual DNA detection at the gas/liquid and liquid/liquid interfaces. A) Image of the purple film formed at the air/water interface after a solution of DNA–AuNPs, target DNA, and F–DNA was allowed to stand for 20 h. B) TEM micrograph of AuNPs sampled at the air/water interface after the addition of DNA–AuNPs, target DNA, and F–DNA. C) TEM micrograph of AuNP networks sampled at the air/water interface after a solution of DNA–AuNPs, target DNA, and F–DNA was allowed to stand for 20 h. Reaction conditions used to generate the data in (A), (B), and (C): DNA–AuNPs (200 μL), target DNA (3.07 μM, 2.5 μL), F–DNA (1.84 μM, 2.5 μL). D) Image of the purple film transferred from the air/water interface to the perfluorohexane/water interface, after the aqueous solution had first been allowed to stand for 5 h before perfluorohexane was added. Reaction conditions: DNA–AuNPs (400 μL), target DNA (3.07 μM, 5 μL), F–DNA (1.84 μM, 5 μL), perfluorohexane (400 μL). The perfluorohexane phase is at the bottom of the vial. All the hybridization experiments were performed at room temperature.

Control experiments indicate that both the target DNA and the fluorous tag are essential components driving the interfacial assembly process, without either of which the solution remains red throughout the process (see Figure S5 in the Supporting Information). Whereas the networked AuNP structures could be disrupted by heating the solution to an elevated temperature, they could be restored upon cooling the solution to room temperature (see Figure S5 in the Supporting Information). The assembly of AuNPs could be accelerated by a freeze-thaw procedure, which is analogous to that from an earlier report.[8] Upon freezing, aggregation of AuNPs occurs immediately, as exemplified by the blue color, which can be accounted for by the high local effective molarities of salts and other components created within the ice (see Figure S6 in the Supporting Information).[8] Remarkably, a purple-colored film could be observed by thawing the solution for only 15 min at room temperature (see Figure S6 in the Supporting Information).

We were encouraged by these initial results and next examined the possibility of inducing the assembly of AuNPs at the interface between water and other phases. Indeed, if perfluorohexane is added before the hybridization, upon prolonged standing, purple films could be discerned at both the air/water and fluorous solvent/water interfaces (see Figure S7 in the Supporting Information). However, after the formation of the purple film at the air/water interface, the addition of perfluorohexane induces transfer of the film to the fluorous solvent/water interface (Figure 2D), suggesting the

preferential interaction of the fluorous tag with fluorous solvent and amphiphilicity of the sandwiched structure.

The successful demonstration of the fluorous-interaction-driven interfacial assembly of AuNPs prompted us to test the feasibility of employing a substrate modified with a fluorous molecule for anchoring these network structures, which is important for the development of a multiplexing assay format. Previously documented array strategies typically involve multistep, complex procedures for the fabrication of surface-bound recognition elements,[24,27] whereas for the aggregation spot test on a reverse-phase thin-layer chromatography (RP/TLC) plate, signal amplification cannot be performed because of the high background signal associated with the porous support (see Figure S8 in the Supporting Information). We envisioned that a combination of advantages from both perspectives would be beneficial. The fluorination of the glass slide was achieved by derivatization with a fluoroalkylsilane molecule. When solutions were used that were similar to those used for experiments involving the air/water and perfluorohexane/water interfaces (DNA–AuNPs, F–DNA, target DNA), the solution appeared purple when placed on the slide, which is in contrast to the red color observed in the absence of the target (Figure 3A). The purple film remained robustly retained on the glass slide after the removal of the solution containing the hybridized structures and the repeated buffer washes. At a higher target-DNA concentration, a blue spot is developed upon drying the slide under a stream of argon gas that can be used as a convenient handle for target identification (see Figure S9 in the Supporting Information). The dehydration-induced color change is likely caused by the change of both the interparticle distance and the surrounding dielectric constant in the solvent-free state. The color intensity of the dried spot is a function of target-DNA concentration, thereby verifying DNA hybridization as the driving force behind this interfacial assembly process. A detection limit of 30.7 nM could be achieved with this assay format (Figure 3B). Acceleration of the assaying process could be equally well effected by a freeze-thaw step before transferring the hybridization solution onto the solid support (see Figure S10 in the Supporting Information). Therefore, with this protocol, we could essentially accomplish target detection within one hour. Once confined to the surface and dehydrated, the AuNP assembly is stable to heating at elevated temperatures in buffer solutions (see Figure S11 in the Supporting Information). This stability is derived, at least in part, from the extensive cross-linking and hydrophobicity of the networked structure. Indeed, scanning electron microscopy (SEM) revealed the existence of a densely packed AuNP network over an extended area (Figure 3C), and the contact angle of water on this spot is only slightly lower than that of the surrounding fluorinated area (see Figure S12 in the Supporting Information). As such, this type of structure is distinctly different from those produced from pure oligonucleotide-modified AuNPs and can be used in situations where more stringent environments (e.g., high temperature) are required. The robust attachment of the AuNP assembly to the glass slide allows for the signal amplification by silver staining, which can markedly enhance the sensitivity (Figure 3D). In this way, a spot that was originally indiscernible could be readily identified (Figure 3B,D; compare the spots marked d in the respective panels). Analysis of the spot with imaging software could provide quantitative correlation between the concentration and the spot intensity (see Figure S13 in the Supporting Information). Although the ultimate detection limit is not yet known, the hybridization signal could be reproducibly resolved at target concentrations as low as 10 pM (equivalent to a sensitivity of 10 attomole) under unoptimized conditions (see Figure S14 in the Supporting Information). Therefore, the sensing performance of our platform is three or four orders of magnitude more sensitive than the homogeneous aggregation-derived methods[8,10,11] by virtue of its amenability to silver signal amplification. Indeed, simultaneous AuNP assembly and surface/interfacial confinement is a unique feature that distinguishes our system from other aggregation structures and presents distinct assay advantages.

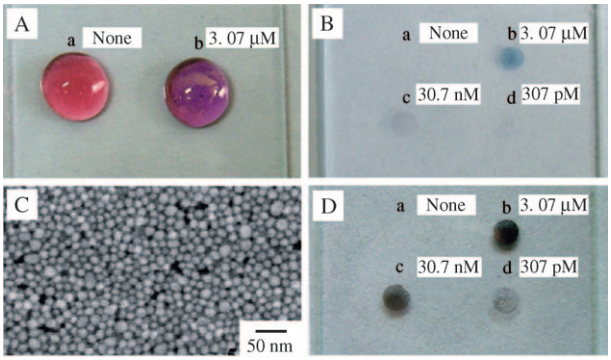

Figure 3. Visual DNA spot test at the solid/liquid interface (hydrated) and on a solid substrate (dehydrated). All the solutions used contained DNA–AuNPs (50 μL in (A), 2 μL in (B), (C), and (D)), F–DNA (1.84 μM, 2 μL), and different amounts of target DNA (1 μL solution); the concentrations of the solutions containing the target DNA are indicated in the figure. A) Image of the solution spotted onto a fluorinated glass slide after being allowed to stand for 20 h. B) Image of the dried spots generated by spotting the solutions onto a fluorinated glass slide and allowing them to stand for 20 h. C) SEM micrograph of a dried spot generated on a fluorinated silicon wafer. D) Image of the dried spots after the exposure of a glass slide, identical to that in (B), to a silver staining solution for 3 min. All the hybridization experiments were performed at room temperature.

To further prove the utility of the method, we carried out experiments demonstrating the ability to differentiate between a fully complementary target and DNA strands with mismatches. The initial experiment was performed by using an oligonucleotide of randomized sequence as the negative control. Under the experimental conditions employed herein, this mismatched DNA is not capable of hybridizing with either DNA–AuNPs or F–DNA. Indeed, at room temperature a clear blue spot could be visualized for the target-DNA strand, whereas no discernible signal could be identified in the negative control sample (Figure 4A). With this promising result in hand, we next evaluated the single-nucleotide-mismatch discrimination capability of the solid support approach. We reasoned that discrimination of a single nucleotide mismatch could be effected by the resolution of AuNP assembly process through exquisitely selected experimental parameters. One such parameter is the hybridization

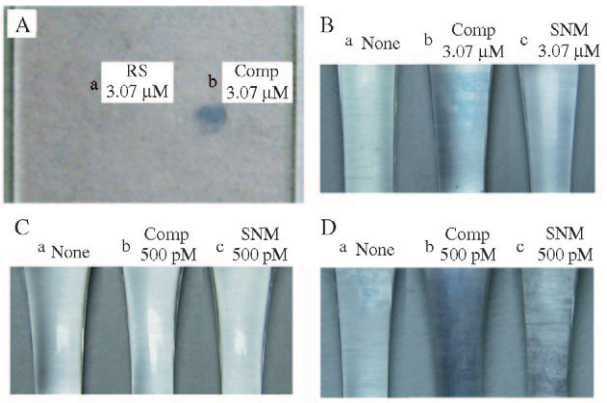

Figure 4. Differentiation of perfectly matched target DNA from DNA strands having mismatches. A) Spot test showing the discrimination of the complementary (Comp) target from an oligonucleotide of a randomized sequence (RS; 3′-GGA TTA TTG TTA AAT ATT GAT AAG GAT-5′). The solutions each contained DNA–AuNPs (2 μL), F–DNA (1.84 μM, 2 μL), and either the a) mismatched DNA (3.07 μM, 1 μL) or b) complementary DNA (3.07 μM, 1 μL). The solutions were allowed to react at room temperature for 20 h. B) Single-nucleotide-mismatch (SNM) differentiation at a higher target concentration. A fluorinated glass rod was immersed in a solution, maintained at 41 °C, for 30 min. The solutions each contained DNA–AuNPs (50 μL), F–DNA (1.84 μM, 2 μL), and either a) 0.3 M PBS buffer (1 μL), b) complementary DNA (3.07 μM, 1 μL), or c) mismatched DNA (3.07 μM, 1 μL). C) A failed test for single-nucleotide-mismatch differentiation at a lower target concentration. A fluorinated glass rod was immersed in a solution, maintained at 41 °C, for 30 min. The solutions each contained DNA–AuNPs (50 μL), F–DNA (1.84 μM, 2 μL), and either a) 0.3 M PBS buffer (1 μL). b) complementary DNA (500 pM, 1 μL), or c) mismatched DNA (500 pM, 1 μL). D) Silver staining of glass rods, which are identical to those in (C), allows differentiation of the single nucleotide mismatch at a lower target concentration. The silver staining was carried out three times, each for 3 min. For (B), (C), and (D), the sequence of the DNA with single nucleotide mismatch is 3′-TAG GAA TAG TTA CAAATT GTT ATT AGG-5′.

temperature, the stringent control of which could be ensured by a PCR machine. After the hybridization solutions had been allowed to stand at 41 °C for 30 minutes in the presence of 3.07 μM target DNA, the distinct blue-colored film could be clearly identified on the immersed glass rod (Figure 4B). At lower concentrations, however, the attached AuNPs could not be visualized (Figure 4C). Again, silver staining could be employed to facilitate the signal readout, which permits the discrimination of a fully complementary target from a strand with single nucleotide mismatch (Figure 4D).

In summary, a versatile method for the interfacial assembly of nanoparticles has been developed. The method features the combination of nature-derived assembly approach (DNA hybridization) and artificially designed binding strategy (fluorous interactions). The AuNP aggregation affords either a distinctive purple film or a dehydrated, visually discernible spot, allowing the facile identification of target DNA. Importantly, one could in principle extend the methodology to a vast range of analytes by substituting the oligonucleotide portions of the two probes with desired structures having the appropriate recognition sites for an intended target.

Received: September 21, 2009
Published online: November 12, 2009

Keywords: DNA detection · fluorous tags · nanoparticles · gold · interfaces

[1] C. T. Caskey, *Science* **1987**, *236*, 1223.
[2] A. Mayer, S. Neuenhofer, *Angew. Chem.* **1994**, *106*, 1097; *Angew. Chem. Int. Ed. Engl.* **1994**, *33*, 1044.
[3] A. F. Johnson, M. D. Struthers, K. B. Pierson, W. F. Mangel, L. M. Smith, *Anal. Chem.* **1993**, *65*, 2352, and references therein.
[4] M. U. Kopp, A. J. de Mello, A. Manz, *Science* **1998**, *280*, 1046.
[5] A. Sassolas, B. D. Leca-Bouvier, L. J. Blum, *Chem. Rev.* **2008**, *108*, 109.
[6] N. L. Rosi, C. A. Mirkin, *Chem. Rev.* **2005**, *105*, 1547.
[7] F. Qiu, D. Jiang, Y. Ding, J. Zhu, L. L. Huang, *Angew. Chem.* **2008**, *120*, 5087; *Angew. Chem. Int. Ed.* **2008**, *47*, 5009.
[8] R. Elghanian, J. J. Storhoff, R. C. Mucic, R. L. Letsinger, C. A. Mirkin, *Science* **1997**, *277*, 1078.
[9] J. J. Storhoff, R. Elghanian, R. C. Mucic, C. A. Mirkin, R. L. Letsinger, *J. Am. Chem. Soc.* **1998**, *120*, 1959.
[10] K. Sato, K. Hosokawa, M. Maeda, *J. Am. Chem. Soc.* **2003**, *125*, 8102.
[11] H. Li, L. Rothberg, *Proc. Natl. Acad. Sci. USA* **2004**, *101*, 14036.
[12] J. M. Nam, K. J. Jang, J. T. Groves, *Nat. Protoc.* **2007**, *2*, 1438.
[13] C. Guarise, L. Pasquato, V. de Filippis, P. Scrimin, *Proc. Natl. Acad. Sci. USA* **2006**, *103*, 3978.
[14] J. Liu, Y. Lu, *J. Am. Chem. Soc.* **2003**, *125*, 6642.
[15] Z. Wang, R. Levy, D. G. Fernig, M. Brust, *J. Am. Chem. Soc.* **2006**, *128*, 2214.
[16] M. S. Han, A. K. R. Lytton-Jean, B.-K. Oh, J. Heo, C. A. Mirkin, *Angew. Chem.* **2006**, *118*, 1839; *Angew. Chem. Int. Ed.* **2006**, *45*, 1807.
[17] D. Möbius, *Acc. Chem. Res.* **1981**, *14*, 63.
[18] M. Sastry, M. Rao, K. N. Ganesh, *Acc. Chem. Res.* **2002**, *35*, 847.
[19] J. J. Storhoff, C. A. Mirkin, *Chem. Rev.* **1999**, *99*, 1849.
[20] U. Feldkamp, C. M. Niemeyer, *Angew. Chem.* **2006**, *118*, 1888; *Angew. Chem. Int. Ed.* **2006**, *45*, 1856.
[21] N. L. Pohl, *Angew. Chem.* **2008**, *120*, 3930; *Angew. Chem. Int. Ed.* **2008**, *47*, 3868.
[22] W. Zhang, *Chem. Rev.* **2004**, *104*, 2531.
[23] S. M. Brittain, S. B. Ficarro, A. Brock, E. C. Peters, *Nat. Biotechnol.* **2005**, *23*, 463.
[24] T. A. Taton, C. A. Mirkin, R. L. Letsinger, *Science* **2000**, *289*, 1757.
[25] J. M. Nam, S. I. Stoeva, C. A. Mirkin, *J. Am. Chem. Soc.* **2004**, *126*, 5932.
[26] X. Zhao, R. Tapec-Dytioco, W. Tan, *J. Am. Chem. Soc.* **2003**, *125*, 11474.
[27] L. A. Chrisey, G. U. Lee, C. E. O'Ferrall, *Nucleic Acids Res.* **1996**, *24*, 3031.

